Received: 25 September 2023 | Accepted: 9 February 2024

DOI: 10.1097/HEP.0000000000000831

ORIGINAL ARTICLE

OPEN

Mesenchymal stem cells alleviate mouse liver fibrosis by inhibiting pathogenic function of intrahepatic B cells

Xudong Feng[1] | Bing Feng[1] | Jiahang Zhou[1] | Jinfeng Yang[1] | Qiaoling Pan[1] | Jiong Yu[1] | Dandan Shang[2] | Lanjuan Li[1,2,3,4] | Hongcui Cao[1,3,5]

[1]State Key Laboratory for the Diagnosis and Treatment of Infectious Diseases, National Clinical Research Center for Infectious Diseases, The First Affiliated Hospital, Zhejiang University School of Medicine, Hangzhou City, China

[2]Jinan Microecological Biomedicine Shandong Laboratory, Jinan City, China

[3]Collaborative Innovation Center for Diagnosis and Treatment of Infectious Diseases, Hangzhou City, China

[4]National Medical Center for Infectious Diseases, Hangzhou City, China

[5]Key Laboratory of Diagnosis and Treatment of Aging and Physic-chemical Injury Diseases of Zhejiang Province, Hangzhou City, China

Correspondence
Hongcui Cao, MD, State Key Laboratory for the Diagnosis and Treatment of Infectious Diseases, The First Affiliated Hospital, Zhejiang University School of Medicine, 79 Qingchun Rd., Hangzhou City 310003, China.
Email: hccao@zju.edu.cn

Abstract

Background and Aims: The immunomodulatory characteristics of mesenchymal stem cells (MSCs) make them a promising therapeutic approach for liver fibrosis (LF). Here, we postulated that MSCs could potentially suppress the pro-fibrotic activity of intrahepatic B cells, thereby inhibiting LF progression.

Approach and Results: Administration of MSCs significantly ameliorated LF as indicated by reduced myofibroblast activation, collagen deposition, and inflammation. The treatment efficacy of MSCs can be attributed to decreased infiltration, activation, and pro-inflammatory cytokine production of intrahepatic B cells. Single-cell RNA sequencing revealed a distinct intrahepatic B cell atlas, and a subtype of naive B cells (B-II) was identified, which were markedly abundant in fibrotic liver, displaying mature features with elevated expression of several proliferative and inflammatory genes. Transcriptional profiling of total B cells revealed that intrahepatic B cells displayed activation, proliferation, and pro-inflammatory gene profile during LF. Fibrosis was attenuated in mice ablated with B cells (μMT) or in vivo treatment with anti-CD20. Moreover, fibrosis was recapitulated in μMT after adoptive transfer of B cells, which in turn could be rescued by MSC injection, validating the pathogenic function of B cells and the efficacy of MSCs on B cell-promoted LF progression. Mechanistically, MSCs could inhibit the proliferation and cytokine production of intrahepatic B cells through exosomes, regulating the Mitogen-activated protein kinase and Nuclear factor kappa B signaling pathways.

Conclusions: Intrahepatic B cells serve as a target of MSCs, play an important role in the process of MSC-induced amelioration of LF, and may provide new clues for revealing the novel mechanisms of MSC action.

Abbreviations: Ccl2, C-C motif chemokine ligand 2; CCl_4, carbon tetrachloride; DAB, 3,3′-diaminobenzidine; DEG, differentially expressed gene; Exo^{MSC}, MSC-derived exosomes; LF, Liver fibrosis; MAPK, Mitogen-activated protein kinase; Mdr2, ATP-binding cassette, sub-family B member 4; MSC, mesenchymal stem cell; NF-kappa B, Nuclear factor kappa B; scRNA-seq, Single-cell RNA sequencing; WT, Wild-type.

Supplemental Digital Content is available for this article. Direct URL citations are provided in the HTML and PDF versions of this article on the journal's website, www.hepjournal.com.

INTRODUCTION

Liver fibrosis (LF) typically results from a range of chronic injuries, such as viral hepatitis, NAFLD, alcohol-associated liver disease, autoimmune hepatitis, primary sclerosing cholangitis, and DILI. These injuries can trigger processes such as hepatocyte apoptosis, inflammatory cell recruitment, endothelial barrier damage, and myofibroblast activation.[1] LF can evolve into cirrhosis or HCC, making it one of the major contributors to mortality and responsible for ~2 million deaths worldwide each year.[2] The initiation and maintenance of liver fibrogenesis crucially depend on inflammation, in which several immune cells are activated and release pro-inflammatory cytokines that activate HSCs.[3] Both the innate and adaptive immune systems are pivotal in the regulation of key pathological processes during LF. Previous studies have indicated that hepatic $CD8^+$ T cells mainly demonstrate pro-fibrotic properties,[4] whereas natural killer cells exhibit unique anti-fibrotic capabilities.[5] Other immune cells such as macrophages,[6–8] natural killer T cells,[9,10] $CD4^+$ T cells,[10,11] and dendritic cells[12] play dual roles (pro-fibrotic and anti-fibrotic responses) in both HSC activation and LF.

The innate activity of B cells and their effector functions through cytokine production has gradually attracted attention in the field of liver disease. One hypothesis suggests the involvement of B cells in the pathogenesis of LF. A report conducted on mice showed a decrease in LF when B cells were absent.[13] However, the underlying mechanism remains unidentified. Later, it was found that LF occurs through a mechanism involving HSC-mediated enhancement of innate B cell activity.[14] Furthermore, during chronic fibrotic cholangitis, activated B infiltrates the livers of $Mdr2^{-/-}$ mice, secreting fibrotic TNF-α and other pro-inflammatory cytokines.[15] In NAFLD or NASH, pro-inflammatory B cells accumulate in the livers of mice, driving disease progression.[16,17] Therefore, the development of novel agents targeting intrahepatic B cells is essential for anti-fibrotic therapy.

Mesenchymal stem cells (MSCs), with their immune-regulatory, anti-inflammatory, and immunosuppressive properties, have recently emerged as promising therapy for treating LF and cirrhosis.[18] Previous studies have suggested that MSCs could alleviate LF by increasing IL-4 and promoting mobilization of KCs,[19] or suppressing liver Th17 cells in an indoleamine 2,3-dioxygenase-dependent manner.[20] Whether and how MSCs regulate liver B cell function in LF remains to be elucidated.

Single-cell RNA sequencing (scRNA-seq) has revolutionized our understanding of disease development, allowing us to investigate both homeostatic and pathogenic cell populations with unprecedented resolution. This adds an additional dimension to transcriptomic data compared with traditional methods that analyze bulk cell populations.[21] Hence, in this study, we combined flow cytometry and scRNA-seq technology to reveal the characteristics of intrahepatic B cells and their functional changes after MSC treatment in a carbon tetrachloride (CCl_4)-induced LF mouse model, with the aim of revealing the underlying mechanism by which MSCs treat LF through B cells. Moreover, the exact molecular mechanisms by which MSCs regulate B-cell function were further investigated using in vitro cell culture systems.

METHODS

Mouse model of liver fibrosis

Wild-type (WT) 6–8-week-old male C57BL/6 mice and $Ighm^{em27Cd56}$ mice (μMT) on a C57BL/6 genetic background (GemPharmatech, Nanjing, China) were used. Mice were housed in a specific pathogen-free environment and maintained on a 12 h light/dark cycle with free access to standard mouse chow and water. To induce LF, the mice were administered 2 mL/kg of CCl_4 (Sigma-Aldrich) dissolved in olive oil (v/v, 25%, Sigma-Aldrich) by i.p. injection twice a week for up to 8 weeks. Mice injected with the same dose of olive oil were used as controls. To deplete $CD20^+$ B lymphocytes, male C57BL/6 mice were treated once every 2 weeks with i.v. injections of anti-mouse CD20 monoclonal antibody (clone 18B12, 7.5 μg/g; InvivoGen). The control group received corresponding mouse IgG2a isotype controls. Animal experimental procedures were performed in accordance with the approval of the Animal Care Ethics Committee of The First Affiliated Hospital, Zhejiang University School of Medicine (Approval No. 2020-1088).

Statistical analysis

Data are expressed as mean ± SEM. All statistical analyses were performed using the GraphPad Prism 8 software (GraphPad Inc.). Differences between the 2 groups were evaluated by Student *t* test or Mann-Whitney *U* test if the data were not normally distributed. Statistical evaluation of multiple groups was performed using one-way ANOVA followed by post hoc Tukey test or, if data were not normally distributed, Kruskal-Wallis test followed by Dunn post hoc test. A value of $p < 0.05$ was considered to be statistically significant.

Other materials and methods, including the list of primers in Supplemental Table S1, http://links.lww.com/HEP/I327, and the list of antibodies in Supplemental Table S2, http://links.lww.com/HEP/I327, are described in the Supplemental Materials and Methods, http://links.lww.com/HEP/I328.

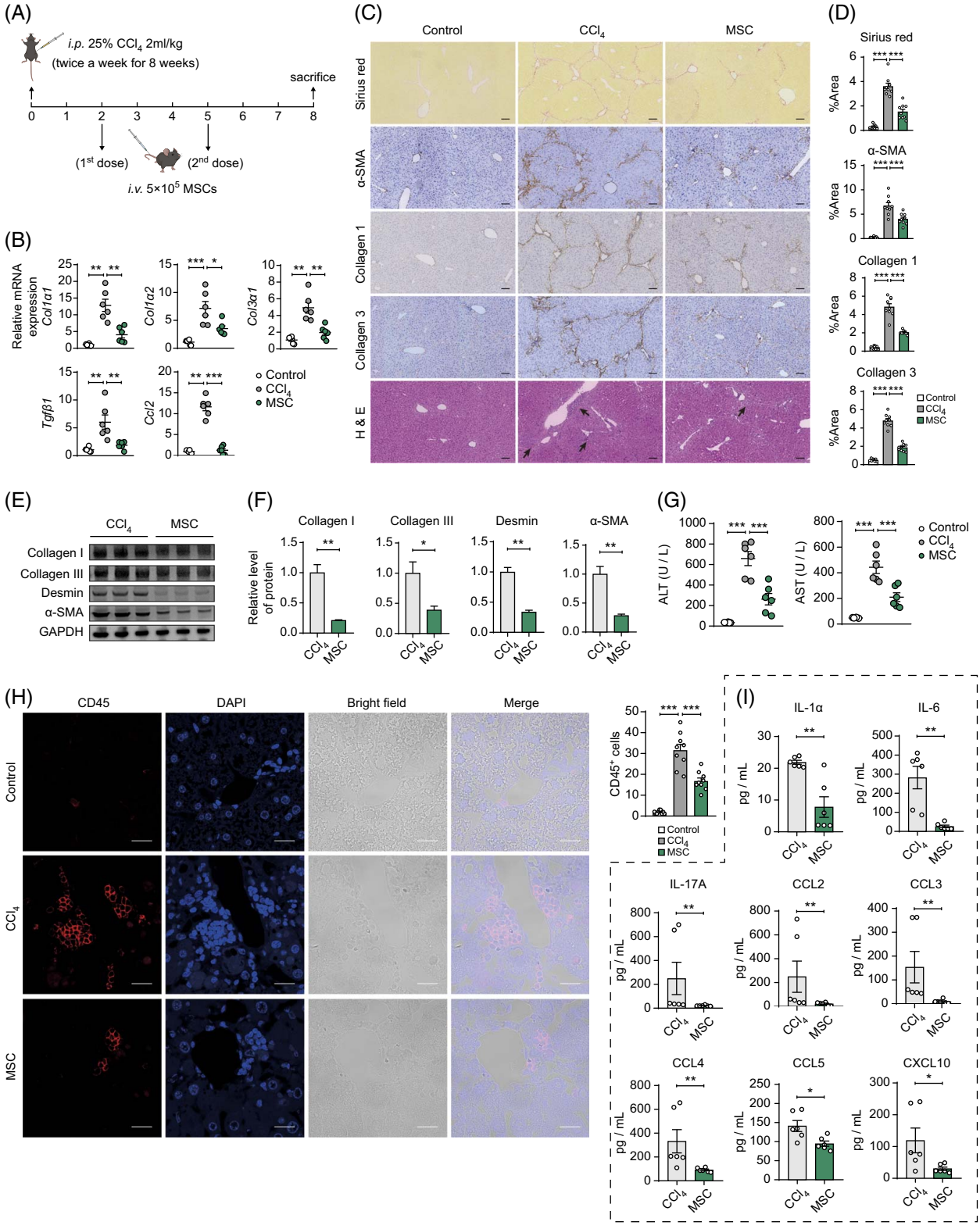

FIGURE 1 MSCs ameliorated CCl_4-induced LF. (A) Schematic diagram of CCl_4-induced LF model and MSC treatment strategy. (B) Quantitative analysis of profibrogenic factors *Col1α1*, *Col1α2*, *Col3α1*, *Tgfβ1*, and *Ccl2* was conducted using qRT-PCR on whole-liver tissue (n = 6 for each group). (C) Representative images from Sirius red, α-SMA, Collagen 1, Collagen 3, and H&E stainings (the arrows indicate clusters of inflammatory cells) on liver sections from different groups (Scale bar: 100 μm). (D) Quantification of histological changes by morphometric pixel analysis (n = 9 for each group; representative of at least 3 independent mice). (E) Western blot analysis of protein levels of Collagen 1, Collagen 3, Desmin, and α-SMA in liver tissues from CCl_4 and MSC-treated mice. (F) Quantification of protein levels in (E) (n = 3 for each group). (G) Serum ALT and AST in Control, CCl_4, and MSC group. (H) Immunofluorescence detection (Scale bar: 20 μm) and quantification of $CD45^+$ cells in Control, CCl_4, and MSC groups. Quantification was based on the number of $CD45^+$ cells infiltrating around the blood vessels in each field of

view (n = 9). (I) Serum concentration of IL-1α, IL6, IL-17A, CCL2, CCL3, CCL4, CCL5, and CXCL10 measured by LEGENDplex™ multi-analyte flow assay (n = 6 for each group). All data were presented as mean ± SEM. *$p < 0.05$, **$p < 0.01$, ***$p < 0.001$. Abbreviations: ALT, alanine aminotransferase; AST, aspartate aminotransferase; α-SMA, α-smooth muscle actin; CCl_4, carbon tetrachloride; CXCL10, C-X-C motif chemokine ligand 10; Ccl2, C-C motif chemokine ligand 2; Col1α1, collagen type I alpha 1 chain; Col1α2, collagen type I alpha 2 chain; Col3α1, collagen type III alpha 1 chain; H&E, hematoxylin and eosin; LF, liver fibrosis; MSC, mesenchymal stem cell; Tgfβ1, transforming growth factor beta 1.

RESULTS

MSCs ameliorated CCl_4-induced LF

A progressive LF model was established in C57BL/6 mice by repeated i.p. injections (twice a week) of CCl_4 for up to 8 weeks. To evaluate the effect of MSCs on LF, we administered MSC concurrently with the induction of fibrosis (Figure 1A). From in vivo fluorescence imaging, the fluorescence intensity of DiR (used to label MSCs) in the liver gradually decreased over time and almost disappeared around day 21 post-injection (Supplemental Fig. S1, http://links.lww.com/HEP/I329). MSC treatment decreased the expression of several liver fibrogenic markers and profibrogenic factors, including collagen type I alpha 1 chain, collagen type I alpha 2 chain, collagen type III alpha 1 chain, TGF beta 1 (*Tgfβ1*), and C-C motif chemokine ligand 2 (*Ccl2*) (Figure 1B). Moreover, mice infused with MSCs exhibited decreased liver scarring, reduced myofibroblast activation (indicated by α-smooth muscle actin), and lower levels of collagen deposition than the untreated groups (Figure 1C, D). Western blot results for the protein levels of collagen 1, collagen 3, and HSC activation markers (desmin and α-smooth muscle actin) also showed consistent trends (Figure 1E, F). Based on the results of liver enzyme indicators (alanine aminotransferase and aspartate aminotransferase), it was indicated that the MSC group exhibited less liver damage (Figure 1G). In the fibrotic liver, significant infiltration of CD45-positive immune cells was observed around the venous blood vessels, a phenomenon that was substantially attenuated in MSC-treated group (Figure 1H). In line with the lymphocyte infiltration phenotype, the MSC infusion group demonstrated decreased levels of serum inflammatory cytokines such as IL-1α, IL6, and IL-17A as well as reduced levels of pro-inflammatory chemokines including CCL2, CCL3, CCL4, CCL5, and C-X-C motif chemokine ligand 10 (Figure 1I). These findings indicate that MSCs can inhibit myofibroblast activation, collagen deposition, and inflammation, thereby delaying the progression of CCl_4-induced LF.

In addition, the methionine-choline-deficient diet-induced NASH mouse model, which is known to progress to fibrosis at later stages, was also utilized to further validate our conclusions. With the application of MSC treatment in this model, effects similar to those observed in the CCl_4-induced model were noted (Supplemental Fig. S2, http://links.lww.com/HEP/I329). These findings indicate the efficacy of MSC therapy in mitigating fibrosis, not only in CCl_4-induced liver injury but also in diet-induced NASH scenarios.

MSC treatment suppressed B cell infiltration and phenotypic activation during LF progression

We further analyzed the characteristics of B cells infiltrating the liver. Both the proportion and absolute number of B cells were markedly increased in the liver of CCl_4-treated group compared with the control group. In mice treated with MSCs, the population of intrahepatic B cells was significantly reduced compared to that in CCl_4-treated mice (Figure 2A-C; Supplemental Fig. S3, http://links.lww.com/HEP/I329). In normal liver tissue, our immunohistochemical analysis revealed a sparse distribution and infrequent B-cell appearance. In the fibrotic liver, however, there was a notable increase in B cells, predominantly clustering around vascular areas. Treatment with MSCs led to a reduction in these B-cell clusters, indicating decreased infiltration in the liver (Figure 2D). Furthermore, in the CCl_4-treated group, intrahepatic B cells exhibited an elevated state of activation and Ag-presenting capacity, as evidenced by the increased expression of activation and costimulatory markers, such as cell-surface major histocompatibility complex class II, CD40, CD86, and CD20. In contrast, the activation of hepatic B cells appeared to be suppressed in the MSC-treated group (Figure 2E, F). To assess the differences in the expression levels of *Tnf*, *Il6*, *Ccl2*, and *Ccl3* in B cells, we purified different groups of intrahepatic B cells (defined as Control-B, CCl_4-B, MSC-B, respectively). The purity of the sorted cells was greater than 90% (Supplemental Fig. S4, http://links.lww.com/HEP/I329). We found that the mRNA levels of these genes were notably elevated in CCl_4-B compared to those in Control-B. Simultaneously, the expression levels of these genes in the MSC-B group were lower than those in the CCl_4-B group to varying extents (Figure 2G). CCl_4-B cells produced higher levels of cytokines compared to those from healthy mice following stimulation, and this elevated pro-inflammatory cytokine production was reduced by the administration of MSCs to fibrotic mice (Figure 2H). In the methionine-choline-deficient diet-induced NASH model, the infiltration of activated B cells in the liver was also observed. Following MSC treatment, both the infiltration and functional activity of B cells were suppressed. These results indicated a similar effect of MSC treatment on hepatic B cells in different models of liver injury (Supplemental Fig. S5, http://links.lww.com/HEP/I329). Taken together, these results suggest that during fibrosis progression, B cells exhibit a more activated

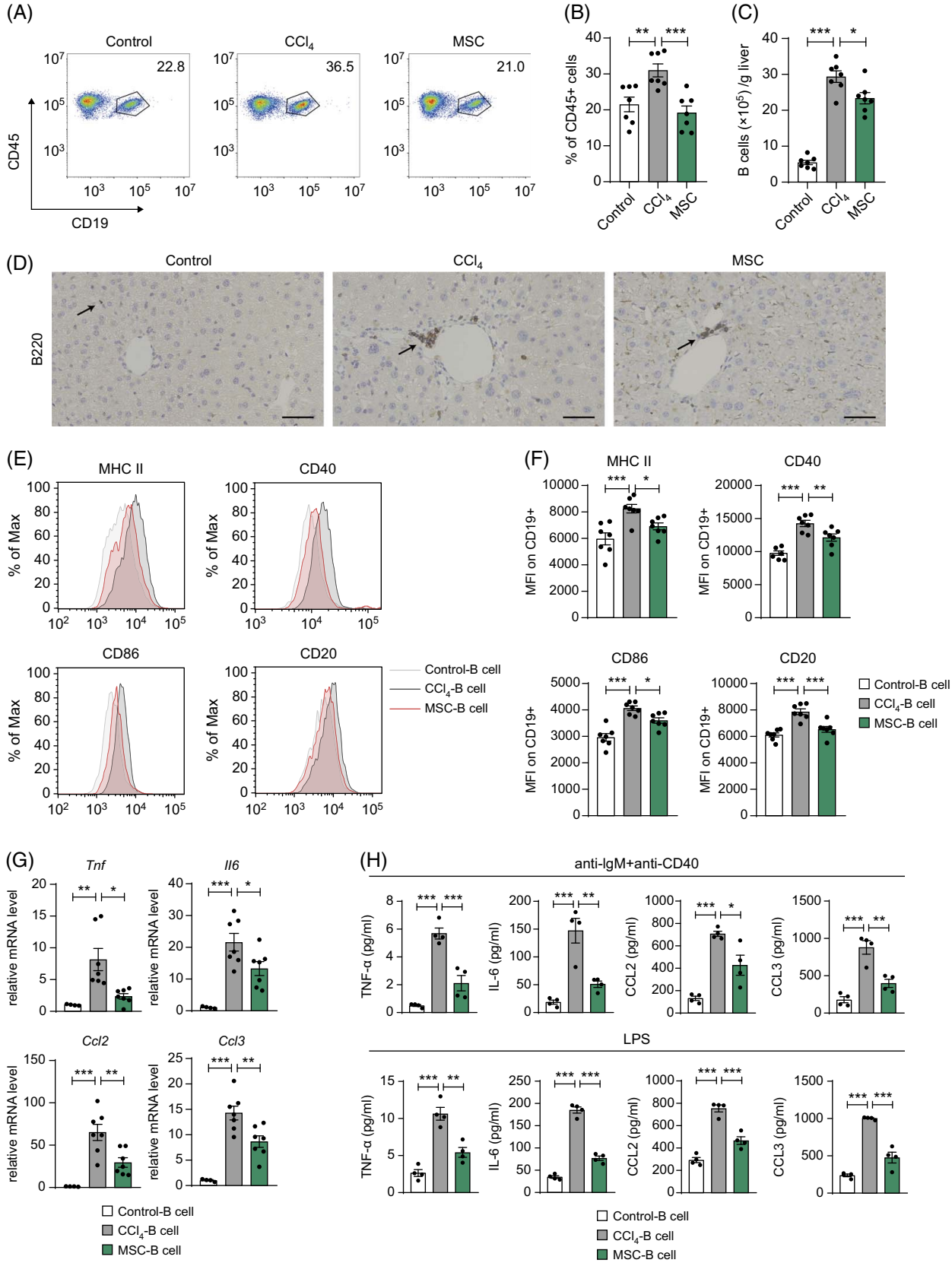

FIGURE 2 MSC treatment suppressed B cell infiltration and phenotypic activation during LF progression. (A) Flow cytometric analysis of intrahepatic B cells. (B) Quantification of the percentages of B cells in hepatic CD45$^+$ cells (n = 7 for each group). (C) Absolute numbers of total B cells (isolated by CD19 microbeads) in the liver from Control, CCl_4, and MSC group (n = 7 for each group). (D) Immunohistochemical analysis of infiltrated B cells in the liver (Scale bar: 50 μm). Arrows in the image point to B220-positive cells identified by immunohistochemical staining. (E)

Representative FACS plots showing expression of activation markers (MHCII, CD40, CD86, and CD20) on gated $CD19^+$ B cells. (F) Quantification of MFI of activation markers (n = 7 for each group). (G) mRNA levels of pro-inflammatory genes (*Tnf*, *Il6*, *Ccl2*, and *Ccl3*) in liver B cells were detected by qRT-PCR (n = 4–7 for each group). (H) B cells extracted from the liver were subjected to in vitro culture under specified stimulation conditions. After 4 days of culture, the supernatants were collected and subjected to analysis using ELISA technique to determine cytokine production (n = 4 for each group). All data were presented as mean ± SEM. *$p < 0.05$, **$p < 0.01$, ***$p < 0.001$. Abbreviations: Ccl2, C-C motif chemokine ligand 2; CCl_4, carbon tetrachloride; LF, liver fibrosis; MFI, mean fluorescence intensity; MHCII, major histocompatibility complex class II; MSC, mesenchymal stem cell.

phenotype and accumulate in the liver with enhanced pro-inflammatory cytokine release and Ag presentation, and more importantly, MSC infusion could suppress this phenomenon efficiently.

Atlas of infiltrated B cells in the liver revealed by scRNA-seq

For in-depth characterization of intrahepatic B cells during CCl_4-induced LF and MSC treatment, we performed scRNA-seq of B cells isolated from healthy, LF, and MSC-treated livers (Figure 3A). The quality control metrics were highly reproducible between individual samples and conditions (Supplemental Fig. S6, http://links.lww.com/HEP/I329). Nine B-cell lineage clusters with distinct transcriptional signatures were identified (Figure 3B-D). By analyzing the expression of known B-cell marker genes, we annotated these 9 subgroups. These included naive B cells expressing *Immunoglobulin heavy constant delta* and *Fc fragment of immunoglobulin M receptor* (Cluster 1–7), unknown B cells with low expression of *Fcmr* (Cluster 8), and plasma cells expressing *Igha* and *Jchain* (Cluster 9) (Figure 3E, F). More than 98% of B cells isolated from the liver were naive B cells. Pseudotime trajectories also showed that the signatures of B cells in the control group were gradually converted to those of the CCl_4 group along the trajectory direction, while those of the MSC group were above the path (Figure 3G). Furthermore, we observed that a subset of naive B cells (clusters 2, 4, and 7) was particularly rare in healthy or MSC-treated liver but abundant in the fibrotic liver (Figure 3H, I). Another part of naive B cells (clusters 1, 3, 5, and 6) showed the opposite trend. Combined with the correlation of the expression profiles of each cluster, we redefined the integration of clusters 1, 3, 5, and 6 as naive B-I and clusters 2, 4, and 7 as naive B-II (Figure 3F, J). The sequential relationship of the B-I and B-II cells was also visualized by mapping them along a pseudo-temporal trajectory (Supplemental Fig. S7A, http://links.lww.com/HEP/I330). The heatmap displayed the genes exhibiting substantially distinct expression patterns among these 2 subsets (Supplemental Fig. S7B, http://links.lww.com/HEP/I330). B-II cells tended to express higher proliferative genes *Fos*, *Myc*, and *Jun* as well as several inflammatory genes *Traf1*, *Cxcr4*, and *H2-Aa* (Supplemental Fig. S7C, http://links.lww.com/HEP/I330; Supplemental Table S3, http://links.lww.com/HEP/I327). Gene enrichment analysis showed that B-II cells were more active relative to B-I cells, as indicated by the upregulation of multiple signaling pathways, notably B cell activation and nuclear factor kappa B (NF-kappa B) signaling pathway (Supplemental Fig. S7D, E, http://links.lww.com/HEP/I330).

MSCs modulated gene profile in intrahepatic B cells during LF, impacting activation, proliferation, and pro-inflammatory patterns

Next, we analyzed the differential expression of genes in total B cells between different groups. After combining B-cell clusters, we detected 1557 differentially expressed genes (DEGs; 732 upregulated and 825 downregulated) between normal and fibrotic livers (Figure 4A; Supplemental Table S4, http://links.lww.com/HEP/I327). The analysis revealed increased expression of proliferative genes (*Fos*, *Jun*, and *Map2k1*) as well as several inflammatory genes (*nfkb1*, *Cxcr4*, *Cxcr5*, *Ccr7*, *H2-Aa*, *Traf4*, and *Tnfaip3*) in the B cells of fibrotic livers (Figure 4B, C; Supplemental Table S4, http://links.lww.com/HEP/I327). Heatmap analysis clearly distinguished B cells in the fibrotic liver from those in the normal liver (Figure 4D). Following this, enrichment analyses were performed on the detected DEGs. The upregulated genes were enriched in terms such as B cell activation, B cell receptor signaling pathway, cell cycle, and positive regulation of B cell proliferation. (Figure 4E). Kyoto Encyclopedia of Genes and Genomes pathway enrichment analysis indicated that the upregulated DEGs were primarily associated with B cell receptor signaling pathway, antigen processing and presentation, leukocyte transendothelial migration, etc. (Figure 4F). Gene Set Enrichment Analysis revealed that the genes in the CCl_4-B cells were active in several pathways, such as B cell activation, B cell proliferation, B cell receptor signaling pathway, Mitogen-activated protein kinase (MAPK) signaling pathway, NF-kappa B signaling pathway, and Toll-like receptor signaling pathway (Figure 4G).

Next, we focused on the DEGs between fibrotic and MSC-treated livers (Figure 4H) to elucidate the modulation of MSCs on B cell gene expression. It was observed that the proliferative gene *Jun* and inflammatory genes *Cxcr4*, *H2- Aa*, *S100a8*, *S100a9*, *Traf4*, *Tnfrsf13c*, and *Traf1* were downregulated in B cells from the MSC-treated liver compared to those from the fibrotic liver (Figure 4B, C;

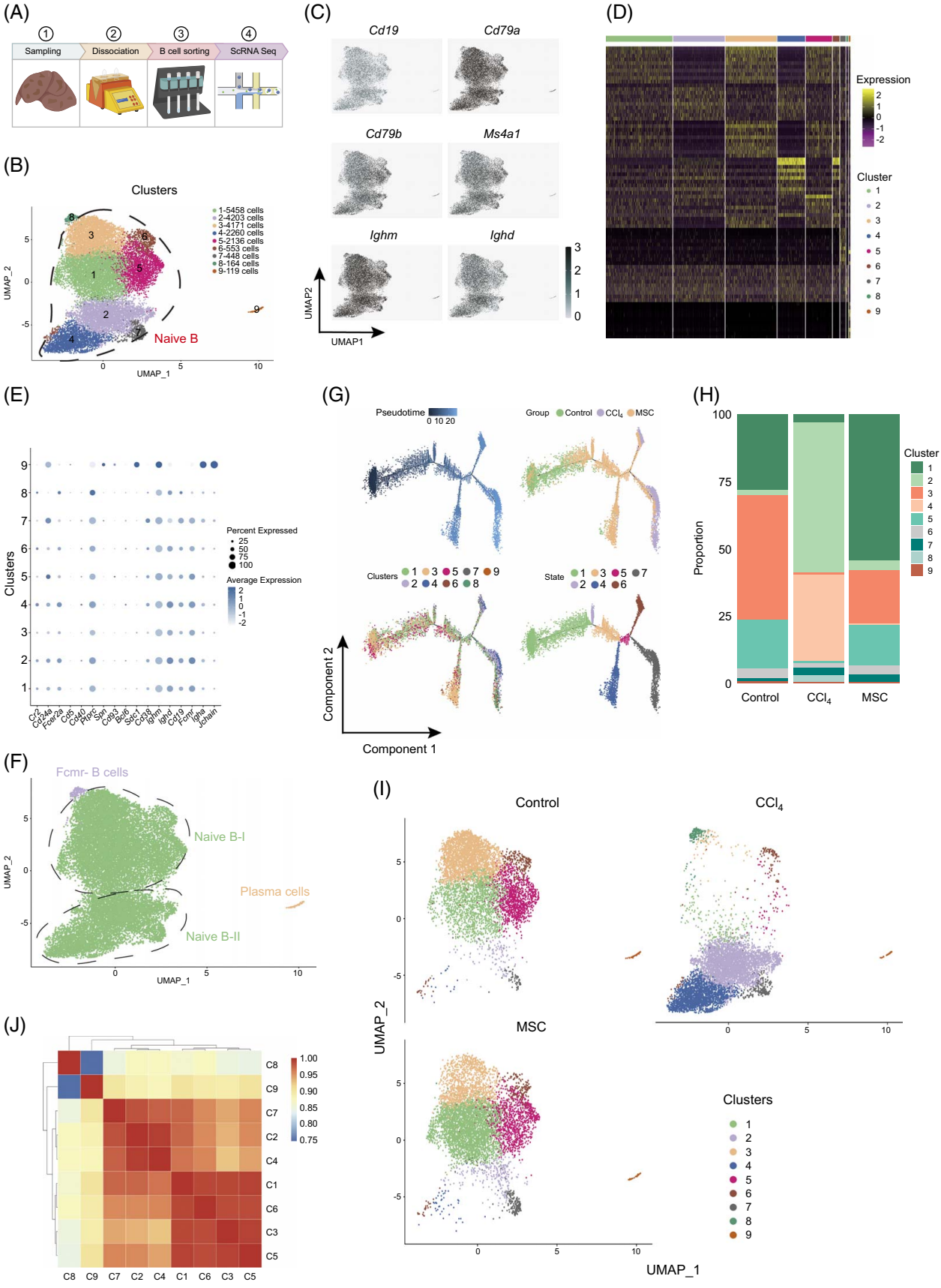

FIGURE 3 Atlas of infiltrated B cells in the liver revealed by single-cell RNA-sequencing. (A) The workflow of scRNA-seq includes liver sampling, liver immune cell isolation, B cell sorting, and sequencing. (B) UMAP map of different scRNA-Seq clusters identified by the graph-based

method. (C) UMAP map of expression of B cells marker genes: *Cd19*, *Cd79a*, *Cd79b*, *Ms4a1*, *Ighm*, and *Ighd*. (D) Top 10 DEGs among nine clusters of the B cells system. (E) Bubble heatmap of the relative expression of selected marker genes for each cluster. (F) UMAP map of redefined B cells. (G) Pseudotime trajectory indicating the development of B cells. The different color schemes represent the segregation based on pseudotime, group, clusters and cell state, respectively. (H) Composition of B cells in each group. (I) UMAP map of clusters in Control, CCl_4, and MSC group. (J) Coefficient heatmap of different clusters. Abbreviations: CCl_4, carbon tetrachloride; DEG, differentially expressed gene; MSC, mesenchymal stem cell; scRNA-seq, Single-cell RNA sequencing; UMAP, Uniform Manifold Approximation and Projection.

Supplemental Table S5, http://links.lww.com/HEP/I327). The downregulated genes in the MSC group were enriched in terms such as response to cytokine, regulation of cell cycle, inflammatory response, chemotaxis, and B cell receptor signaling pathway (Figure 4I). Kyoto Encyclopedia of Genes and Genomes analysis demonstrated that these downregulated DEGs were associated with Ag processing and presentation, protein processing in the endoplasmic reticulum, IL-17 signaling pathway, etc. (Figure 4J). Furthermore, Gene Set Enrichment Analysis showed that B cell activation, B cell proliferation, B cell receptor signaling pathway, MAPK signaling pathway, NF-kappa B signaling pathway, and Toll-like receptor signaling pathway gene sets were inhibited in MSC-B cells (Figure 4K). These findings show that intrahepatic B cells display activation, proliferation, and pro-inflammatory gene profile during LF, but MSC treatment can inhibit the expression of related genes.

B cells were involved in liver fibrogenesis and could serve as target cells for MSCs to exert therapeutic effects

The above evidence showed that B cells displayed phenotypes such as activation, proliferation, and pro-inflammatory activity during LF, but whether there was a direct causal relationship between B cells and the severity of LF was unclear. Therefore, to determine whether B cells played a direct role in the pathogenesis of LF, we assessed the progression of liver fibrogenesis in 8-week CCl_4-treated μMT mice (Figure 5A). μMT mice have a targeted deletion of the Igμ heavy chain,[22] resulting in a lack of mature B cells (Supplemental Fig. S8, http://links.lww.com/HEP/I330). Compared to fibrotic lesions in WT mice, μMT mice exhibited reduced fibrosis (Figure 5B-D). Additionally, we used WT mice depleted of B lymphocytes with a CD20-specific monoclonal antibody[23] as another supporting animal model (Supplemental Fig. S9A, http://links.lww.com/HEP/I331). As anticipated, the administration of the CD20 monoclonal antibody resulted in a persistent and significant decrease in the quantity of mature B lymphocytes in both the liver and spleen (Supplemental Fig. S9B, C, http://links.lww.com/HEP/I331). Similarly, CD20-specific monoclonal antibody-induced B-cell depletion ameliorated inflammation and fibrogenesis during LF (Supplemental Fig. S9D-F, http://links.lww.com/HEP/I331). However, when we transplanted MSCs in the B cell-deficient LF mouse model, no further therapeutic effect of MSCs was observed (Figure 5B-D; Supplemental Fig. S9D-F, http://links.lww.com/HEP/I331). This, to some extent, not only illustrates the key role of B cells in the mechanism of MSC therapy but also indicates that the efficacy of MSC might depend on the injury microenvironment of the liver.

Moreover, the adoptive transfer of B cells from WT spleens to μMT mice aggravated liver injury and fibrosis in CCl_4-treated μMT mice (Figure 5E-H; Supplemental Fig. S10, http://links.lww.com/HEP/I331). Interestingly, MSC treatment could rescue aggravated LF induced by adoptive transfer of B cells, as indicated by the decreased expression levels of several fibrogenic makers after co-injection of MSCs and B cells (Figure 5E-H).

Considering the role of B cells in promoting the advancement of LF, we undertook an initial investigation of the underlying molecular mechanism. Mechanistically, B cells may have effects on liver monocyte/macrophage infiltration in fibrotic mice, as indicated by the reduced frequency and total number of $CD11b^{hi}$ $F4/80^{int}$ mononuclear macrophages in μMT mice compared with WT mice (Supplemental Fig. S11, http://links.lww.com/HEP/I331). Monocytes are acknowledged for their significant involvement in LF after recruitment through CCL2 mediation.[24] To examine the potential of soluble factors produced by activated B cells to directly activate HSCs, we co-cultured primary HSCs with liver B cells through a transwell system. We found that activated B cells could secrete pro-inflammatory factors to activate the JAK-STAT3 pathway in HSCs, leading to their activation (Supplemental Fig. S12, http://links.lww.com/HEP/I332).

MSC-derived secretome mediates the effect of MSCs on B cell function

Given that MSCs could inhibit the function of intrahepatic B cells in vivo, we further explored the underlying mechanism in vitro. We first investigated the effects of MSCs on liver B-cell proliferation upon stimulation with αIgM and αCD40. Hepatic B cells were stained with the cell surface dye 5,6-carboxyfluorescein diacetate succinimidyl ester before stimulation to visualize cell division. As shown in Supplemental Fig. S13A, http://links.lww.com/HEP/I332, the proliferative capacity of stimulated B cells was inhibited when co-cultured with MSCs for 3 days. This conclusion was

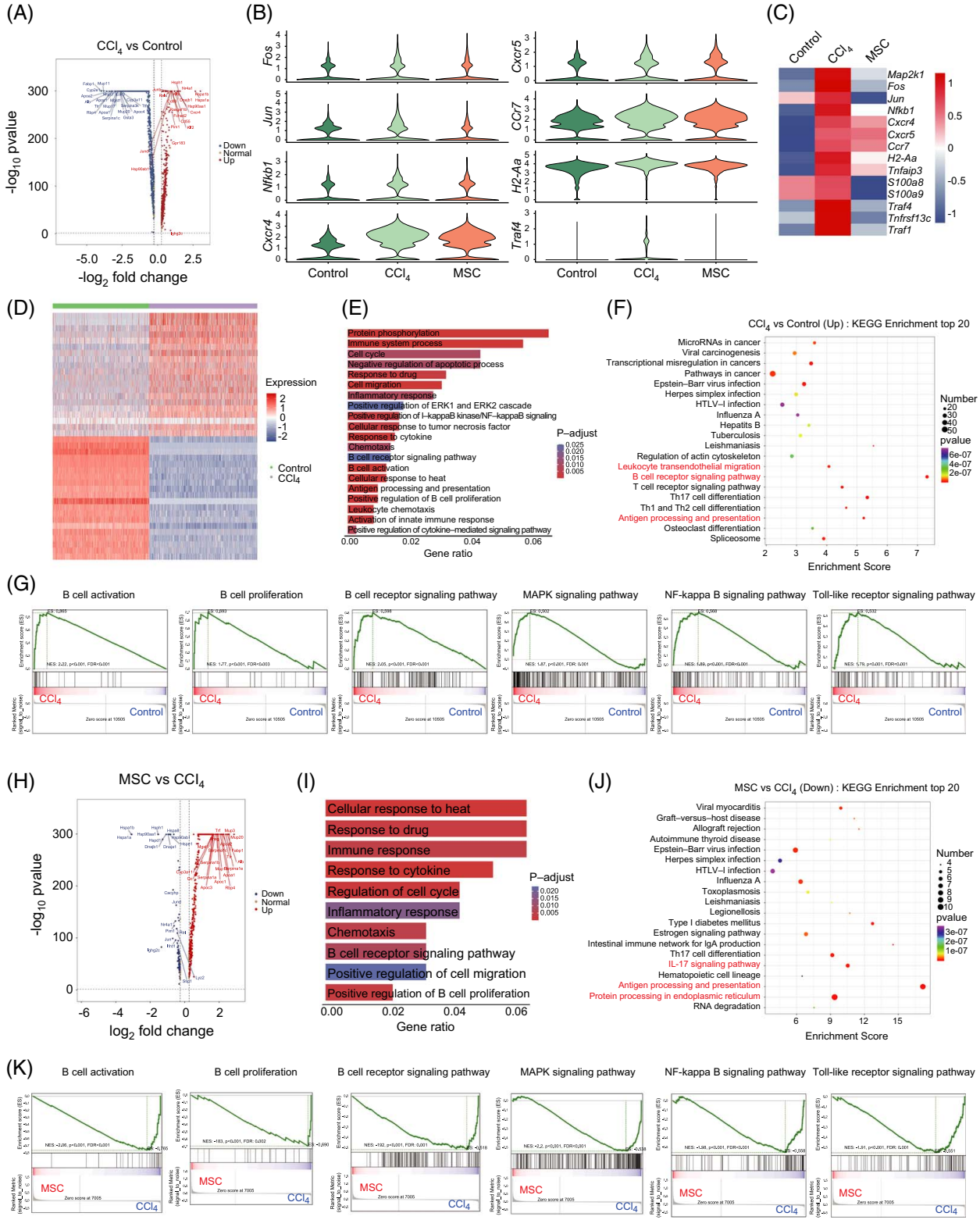

FIGURE 4 MSCs modulated gene profile in intrahepatic B cells during LF, impacting activation, proliferation, pro-inflammatory patterns. (A) Volcano plot for DEGs of total B cells between Control and CCl_4 group. (B) Violin plots showing the log-transformed expression of *Fos*, *Jun*, *Nfkb1*, *Cxcr4*, *Cxcr5*, *CCr7*, *H2-Aa*, and *Traf4*. (C) Heatmap of selected gene expression of total B cells in different groups. (D) Heatmap of all DEGs of total B cells between Control and CCl_4 group. (E) Bar graph showing the functions enriched in upregulated DEGs of B cells in the CCl_4 group. Length represents the gene ratio and color represents the adjusted *p*-value. (F) Top 20 functional enrichment analyses with KEGG analysis using the upregulated DEGs in the CCl_4 group. (G) GSEA between Control and CCl_4 groups. (H) Volcano plot of DEGs in total B cells between CCl_4 and MSC groups. (I) Bar graph showing functions enriched in down-regulated DEGs of B cells in the MSC group. (J) KEGG pathway enrichment analysis of the downregulated DEGs in the MSC group. (K) GSEA analysis between CCl_4 and MSC group. Abbreviations: CCl_4, carbon tetrachloride; DEG, differentially expressed gene; GSEA, Gene Set Enrichment Analysis; KEGG, Kyoto Encyclopedia of Genes and Genomes; LF, liver fibrosis.

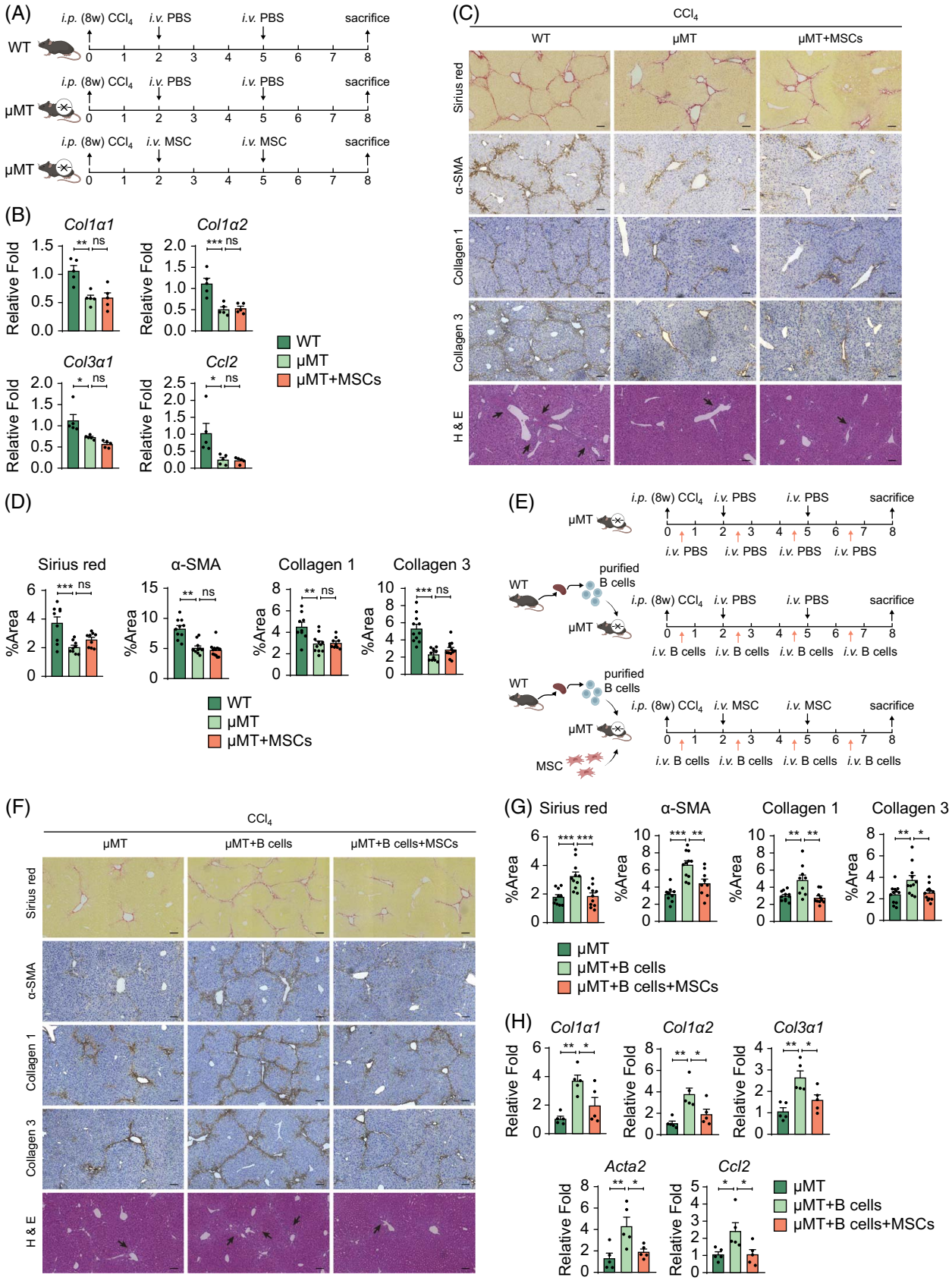

FIGURE 5 B cells were involved in liver fibrogenesis and served as target cells for MSCs to exert therapeutic effects. (A) Schematic representation of the methodology of inducing LF in μMT mice and MSC treatment. (B) Quantitative analysis of profibrogenic factors *Col1α1*, *Col1α2*, *Col3α1*, and *Ccl2* by qRT-PCR on whole-liver tissue (n = 5 for each group). (C) Representative images from Sirius red, α-SMA, collagen 1,

collagen 3, and H&E stainings (the arrows indicate clusters of inflammatory cells) on liver sections of different group (Scale bar: 100 μm). (D) Quantification of stained area in (C) (n = 9–12 for each group; representative of at least 3 independent mice). (E) Schematic diagram of the experimental design for adoptive transfer of B cells during LF inducing. (F) Representative images from Sirius red, α-SMA, collagen 1, collagen 3, and H&E stainings (the arrows indicate clusters of inflammatory cells) of the liver after adoptive transfer of B cells. (G) Quantification of stained area in (F) (n = 9–12 for each group; representative of at least 3 independent mice). (H) mRNA levels of *Col1α1*, *Col1α2*, *Col3α1*, *Acta2*, and *Ccl2* in liver tissue (n = 5 for each group). All data were presented as mean ± SEM. *$p < 0.05$, **$p < 0.01$, ***$p < 0.001$. Abbreviations: α-SMA, α-smooth muscle actin; Ccl2, C-C motif chemokine ligand 2; Col1α1, collagen type I alpha 1 chain; Col1α2, collagen type I alpha 2 chain; Col3α1, collagen type III alpha 1 chain; H&E, hematoxylin and eosin; LF, liver fibrosis; MSC, mesenchymal stem cell.

further confirmed by the total number of suspended cells (Supplemental Fig. S13B, http://links.lww.com/HEP/I332). Cell cycle analysis showed that the proportion of G0/G1-phase cells was smaller in the αIgM/αCD40 group than that in the MSCs group, and the proportion of S-phase cells was larger (Supplemental Fig. S13C, D, http://links.lww.com/HEP/I332). This suggests that the inhibition of liver B-cell proliferation by MSCs is related to cell cycle arrest. Consistent with the above in vivo results, we found that the ability of liver B cells to secrete TNF-α and IL6 was also negatively regulated by MSCs in vitro (Supplemental Fig. S13E, F, http://links.lww.com/HEP/I332). Previous studies have shown that the regulation of immune cells by MSCs could be mediated through cell-cell contacts or the secretome,[25,26] so we next used the transwell co-culture system to explore how MSCs acted on B cells. As shown in Figure 6A and B, even though MSCs and B cells were separated, the inhibitory effect of MSCs on the proliferation of B cells still existed. Compared with the αIgM/αCD40 group, prolonged G0/G1 phase and shortened S and G2/M phases were observed in the MSC group (Figure 6C, D). The mRNA levels of the cell cycle-associated genes *Ccnd2* and *Ccne1* also decreased in the MSC group (Figure 6E). At the same time, MSCs also reduced the protein expression levels of c-Myc, cyclin D2 (CCND2), and cyclin E1 (CCNE1) (Figure 6F). These results indicate that MSCs were still responsible for the cell cycle distribution and progression of B cells in the presence of the filter. Next, we investigated the cytokine production function of B cells. The mRNA levels of *Tnf*, *Il6*, *Ccl2*, and *Ccl3* were significantly upregulated upon stimulation but downregulated in the presence of MSCs (Figure 6G). Similarly, the observed trend in TNF-α and IL6 production by intrahepatic B cells, which increased with stimulation and decreased following culture with MSCs, is consistent with our findings on mRNA expression levels (Figure 6H-J). Taken together, MSC-dependent suppression of intrahepatic B cell function is mediated by its secretome.

Exosomes were key effectors of MSCs to suppress intrahepatic B cell function

MSC-derived secretome consists of a protein-soluble fraction, including growth factors and cytokines, and a vesicular fraction, consisting of microvesicles and exosomes.[27] To confirm whether exosomes in the secretome are involved in the inhibitory effect of MSCs on intrahepatic B cells, we pretreated MSCs with GW4869 to inhibit the release of exosomes (Supplemental Fig. S14A, http://links.lww.com/HEP/I332). MSCs pretreated with GW4869 showed limited potency in suppressing B cell proliferation, cell cycle progression, and pro-inflammatory functions (Figure 7A-D). Next, we extracted MSC-derived exosomes (Exo^{MSC}) to verify the effect of exosomes on B cell function. Exo^{MSC} displayed cup-like morphology with a mode diameter of ~111 nm (Supplemental Fig. S14B, C, http://links.lww.com/HEP/I332) and expressed exosomal markers CD63, HSP70, and HSP90 (Supplemental Fig. S14A, http://links.lww.com/HEP/I332). It was observed that after 12 h of incubation, around 8.35% of B cells exhibited green fluorescence, indicating that Exo^{MSC} might have been taken up by ~8% of B cells (Supplemental Fig. S15A-B, http://links.lww.com/HEP/I332). Exo^{MSC} treatment suppressed B-cell proliferation in the presence of αIgM/αCD40 or lipopolysaccharide (Figure 7E-H). This effect could be dependent on the regulation of the cell cycle, as most (92.05% in αIgM/αCD40 stimulation; 87.76% in lipopolysaccharide stimulation) B cells remained in the G0/G1 phase (Figure 7I-K). We also found that some pro-inflammatory genes (*Tnf*, *Il6*, *Ccl2*, and *Ccl3*) were expressed at lower levels in the Exo^{MSC} group (Figure 7L, M). To confirm this finding, we analyzed the levels of these 4 cytokines in the supernatant of activated B cells isolated from fibrotic liver. We found that intrahepatic B cells in the exosome-treated group produced fewer pro-inflammatory cytokines in response to stimulation (Figure 7N, O).

For B cells, signaling through MAPK and NF-kappa B is indispensable for proper activation, proliferation, and pro-inflammatory cytokine production, as described in the sequencing results above. In stimulated B cells, we detected a robust signal-induced increase in phosphorylated extracellular regulated kinase, phosphorylated Inhibitor of nuclear factor kappa-B kinase subunit alpha/beta, and nuclear P65, but the expression of these proteins was reduced in the presence of exosomes (Figure 8A-D). To conclusively demonstrate that Exo^{MSC} inhibits B cell functions through the MAPK and NF-kappa B signaling pathways, phorbol 12-myristate 13-acetate was utilized to stimulate these pathways. Phorbol 12-myristate 13-acetate activation led to significant upregulation of phosphorylated Inhibitor of nuclear

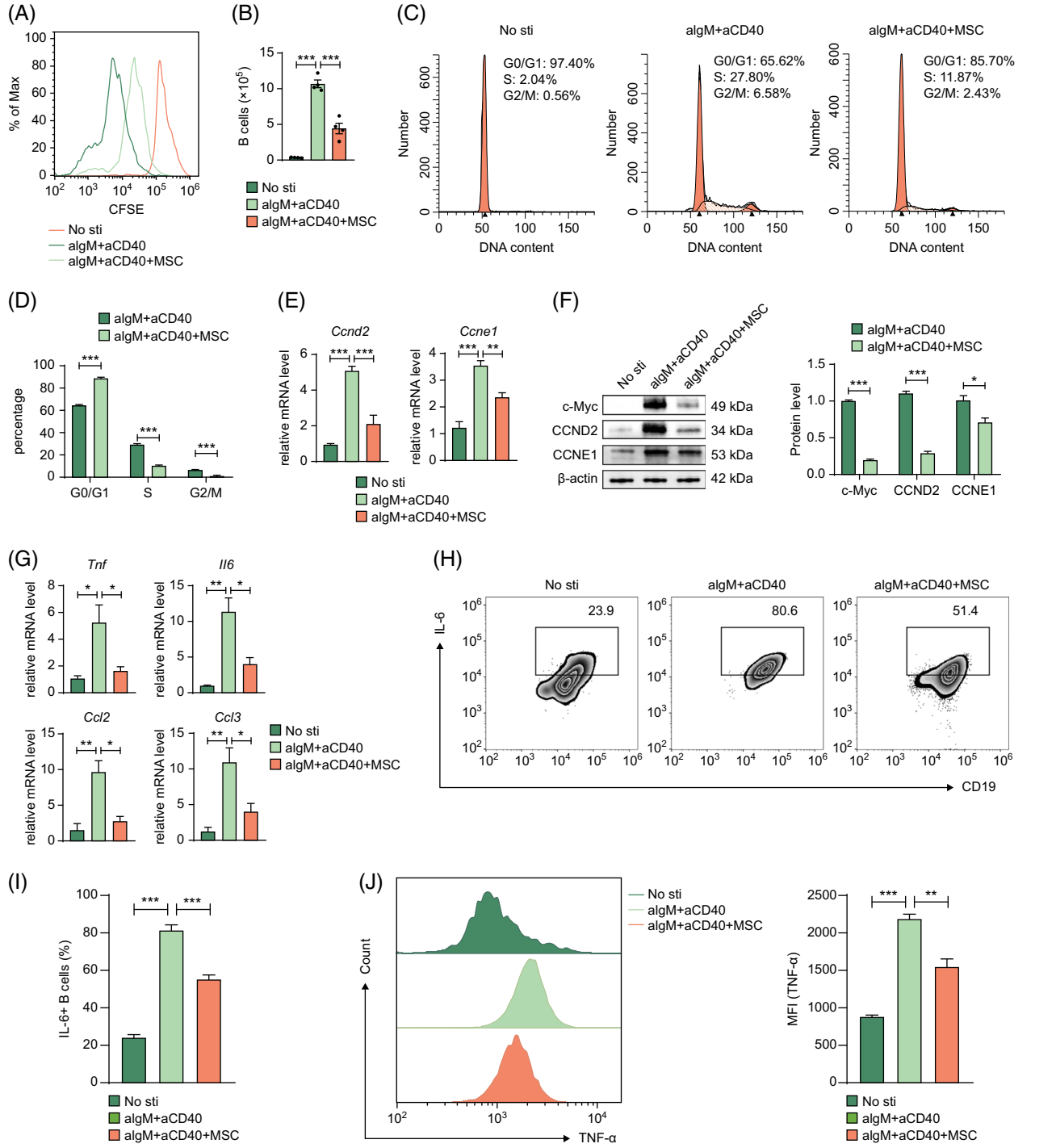

FIGURE 6 MSCs derived secretome mediated the effect of MSCs on B cells function. (A) Residual CFSE fluorescence intensity in CFSE-labelled intrahepatic B cells after 3 days of co-culture with MSC in a transwell system in the presence of stimuli. (B) The total number of B cells collected after 3 days of culture under different culture conditions (n = 4 for each group). (C) Cell cycle phase distribution was measured with flow cytometry after 2 days of culture. (D) Graph of the cell cycle distribution (n = 4 for each group). (E) mRNA levels of *Ccnd2* and *Ccne1* in B cells after co-culture with MSC (n = 3–4 for each group). (F) Western blot of expression levels of c-Myc, CCND2, and CCNE1 in B cells (n = 3 for each group). (G) mRNA levels of pro-inflammatory genes (*Tnf*, *Il6*, *Ccl2*, and *Ccl3*) in liver B cells after co-culture with MSCs (n = 3 for each group). (H) The expression of IL6 protein in cultured B cells was analyzed by FACS. (I) The percentage of IL6$^+$ B cells in different culture conditions (n = 3 for each group). (J) Histograms of TNF-α expression patterns and corresponding MFI analysis in B cells after co-culture with MSCs (n = 3 for each group). All data were presented as mean ± SEM. *$p < 0.05$, **$p < 0.01$, ***$p < 0.001$. Abbreviations: Ccl2, C-C motif chemokine ligand 2; CCND2, cyclin D2; CCNE1, cyclin E1; CFSE, 5,6-carboxyfluorescein diacetate succinimidyl ester; MFI, mean fluorescence intensity; MSC, mesenchymal stem cell.

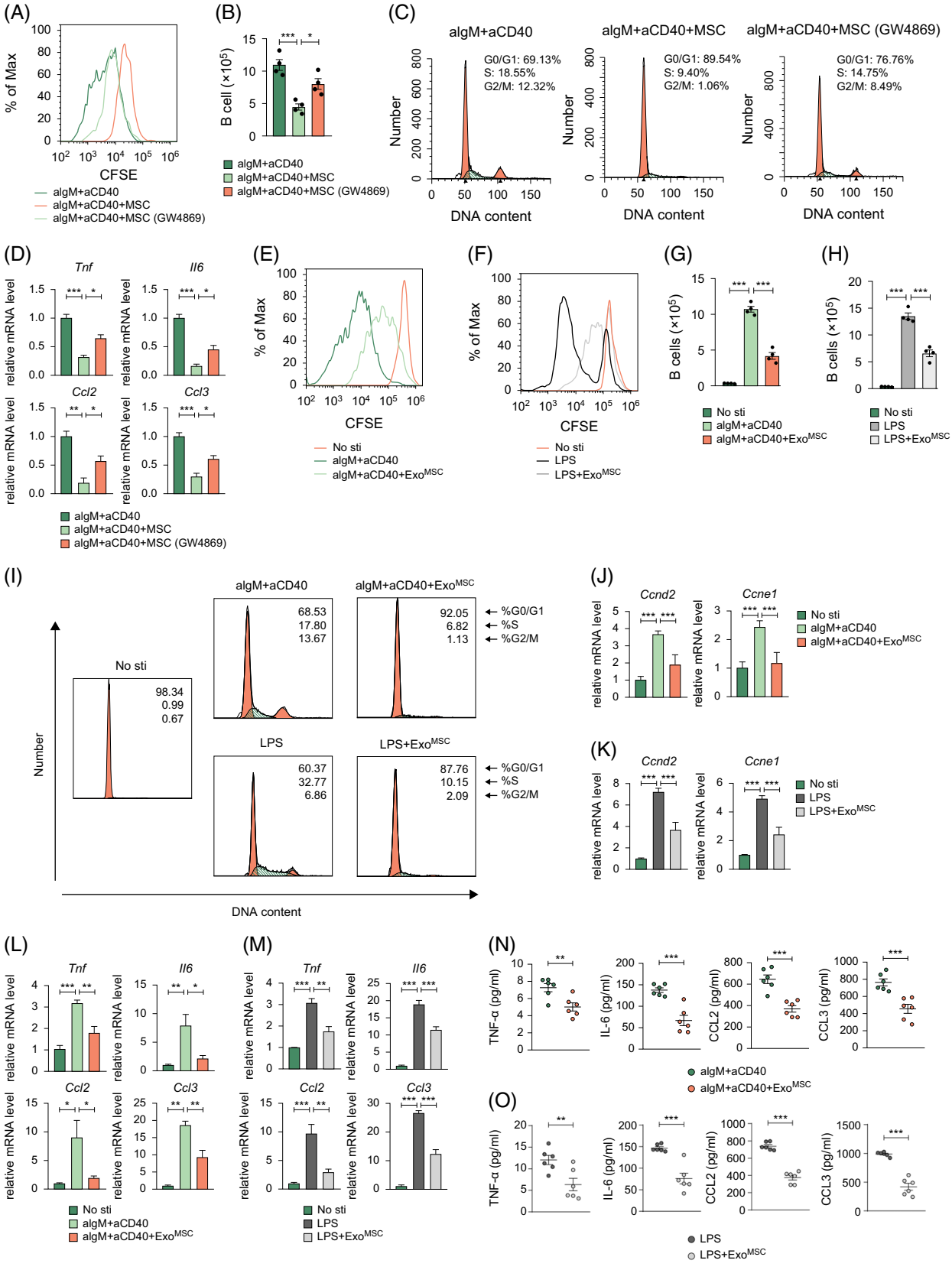

FIGURE 7 Exosomes were key effectors of MSCs to suppress intrahepatic B cells function. (A) CFSE analysis of intrahepatic B cells co-cultured with MSCs pretreated with GW4869 (an exosome release inhibitor) in a transwell system. (B) Total number of B cells collected after 3 days of co-culture with GW4869-pretreated MSCs in a transwell system (n = 4 for each group). (C) Cell cycle phase distribution of B cells after 2 days of co-culture with GW4869-pretreated MSCs in a transwell system. (D) mRNA levels of pro-inflammatory genes (*Tnf*, *Il6*, *Ccl2*, and *Ccl3*) in

liver B cells after co-culture with GW4869-pretreated MSCs (n = 3 for each group). (E, F) CFSE analysis of αIgM/αCD40- or LPS-stimulated intrahepatic B cells after Exo^{MSC} treatment. (G, H) The total number of αIgM/αCD40-stimulated or LPS-stimulated intrahepatic B cells after 3 days of treatment with Exo^{MSC} (n = 4 for each group). (I) Cell cycle analysis of stimulated B cells after Exo^{MSC} treatment. (J, K) *Ccnd2* and *Ccne1* mRNA levels in αIgM/αCD40- or LPS-stimulated B cells after Exo^{MSC} treatment were detected by RT-qPCR (n = 3 for each group). (L, M) mRNA levels of *Tnf*, *Il6*, *Ccl2*, and *Ccl3* in αIgM/αCD40-stimulated or LPS-stimulated liver B cells after Exo^{MSC} treatment (n = 3 for each group). (N, O) ELISA analysis of TNF-α, IL6, CCL2, and CCL3 in the supernatant from αIgM/αCD40-stimulated or LPS-stimulated liver B cells after Exo^{MSC} treatment (n = 6 for each group). All data were presented as mean ± SEM. *$p < 0.05$, **$p < 0.01$, ***$p < 0.001$. Abbreviations: Ccl2, C-C motif chemokine ligand 2; CCND2, cyclin D2; CCNE1, cyclin E1; CFSE, 5,6-carboxyfluorescein diacetate succinimidyl ester; CFSE, 5,6-carboxyfluorescein diacetate succinimidyl ester; Exo^{MSC}, MSC-derived exosomes; LPS, lipopolysaccharide; MSC, mesenchymal stem cell.

factor kappa-B kinase subunit alpha/beta and phosphorylated extracellular regulated kinase 1/2 expression levels (Figure 8E). This upregulation effectively reversed the inhibition triggered by Exo^{MSC}, restoring B cell proliferation and cytokine production functions (Figure 8F-I). This phenomenon suggests that Exo^{MSC} may primarily target upstream molecules in both the MAPK and NF-kappa B signaling pathways. Taken together, these data suggest that exosomes are key effectors of MSC suppression of B cells, which mainly target the MAPK and NF-kappa B signaling pathways.

DISCUSSION

LF occurs due to persistent inflammation and is characterized by alterations in the extracellular matrix with increased deposition of collagen and other fibrillar proteins, like elastin, in the Disse's space.[28] It is well known that LF is a dynamic process that can be effectively reversed, and modulating the liver immune microenvironment is considered a therapeutic strategy for LF.[29] A large amount of preclinical evidence has shown that MSC treatment can improve LF and we also found that MSC treatment has the potential to ameliorate LF by inhibiting both inflammation and fibrogenesis. However, the participation of immune cells in MSC treatment of LF is a dynamic and complex process, and the mechanism of action on immune cells, especially B cells, is still unclear.

B cells are lymphocytes that exhibit remarkable versatility, showcasing a wide array of functions.[30] While the increased versatility of B cells may be advantageous for organs with multiple biological functions, it also comes with potential risks related to higher demands and susceptibility for regulation, especially during periods of imbalance.[14] Intrahepatic B-cell accumulation and activation have been recognized as significant mechanisms contributing to the pathogenesis of NASH, as they promote hepatic glucose intolerance, inflammation, and fibrosis.[17] We found that the proportion and absolute number were markedly increased in the fibrotic liver. Furthermore, liver B cells exhibited an elevated state of activation during LF, marked by the increased expression of activation and costimulatory markers. In fibrotic mice, intrahepatic B cells exhibit a pro-inflammatory gene signature and behavioral pattern, producing TNF-α, IL6, CCL2, and CCL3 in response to stimulation.[14] In purified B cells from fibrotic livers, we observed elevated mRNA expression levels of *Tnf*, *Il6*, *Ccl2*, and *Ccl3* compared to B cells from healthy livers. Concurrently, B cells purified from fibrotic mice exhibited higher production of these cytokines in response to stimulation than B cells from healthy mice. MSCs have been investigated in preclinical and clinical studies as a treatment for immune disorders due to their ability to induce systemic immunosuppression.[31] In this study, MSCs significantly inhibited B-cell function during LF through the reduction of B-cell infiltration, inhibition of their activation, and suppression of pro-inflammatory gene expression. Moreover, administration of MSCs to fibrotic mice impaired the capacity of intrahepatic B cells to produce pro-inflammatory cytokines.

Intrahepatic B cells have been reported to be phenotypically similar to splenic B2 cells (classified according to reaction specificity) but express lower levels of CD23 and CD21 and higher levels of CD5.[13] Barrow et al reported 4 distinct intrahepatic B cell populations, of which the major population consisted of mature B cells expressing increased inflammatory genes during NASH.[17] In the triclosan-induced LF mouse model, naive B cells (classified according to activation stage) accounted for the majority, while memory B cells and plasma cells accounted for less.[32] Our single-cell analysis provided new insights into the heterogeneity of liver B cells in CCl_4-induced LF as well as into the mechanisms by which MSCs affect B cells. We found that B cells in the liver were mainly naive B cells (above 98%), which suggested that liver B cells mainly functioned as innate immune cells in the context of this study, independent of antibody secretion. Interestingly, we identified a distinct subset of naive B cells (B-II), whose relative abundance was dramatically increased in fibrotic liver. This subset of B cells is disease-specific, displaying mature features with elevated expression of several proliferative and inflammatory genes. The results of DEG analysis indicated that B cells displayed an innate-like gene signature with increased expression of *nfkb1*, *Cxcr4*, *Cxcr5*, *Ccr7*, *H2- Aa*, and *Tnfaip3* during LF, as well as several activated pathways, such as B cell activation, B cell proliferation, MAPK signaling pathway, NF-kappa B signaling pathway, and Toll-like receptor signaling pathway. In contrast, B cells from MSC-treated livers exhibited down-regulation of the proliferative gene *Jun* and inflammatory genes *S100a8*, *S100a9*, *Cxcr4*, *H2-*

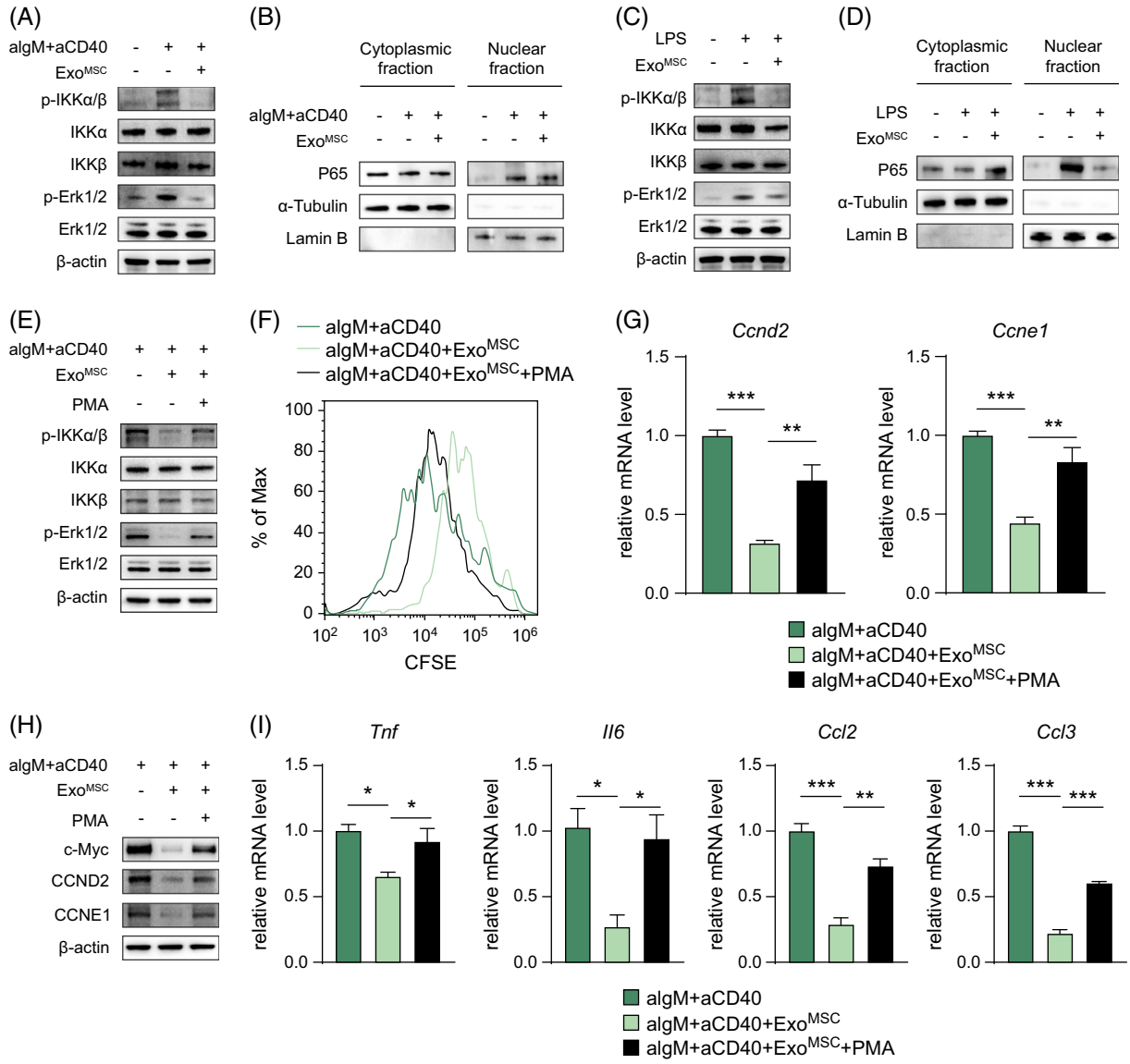

FIGURE 8 Exosomes from MSC modulated intrahepatic B cells function through the MAPK and NF-kappa B signaling pathways. (A) Western blot of p-IKKα/β, IKKα, IKKβ, p-Erk1/2, ERK1/2, and β-actin in αIgM/αCD40-stimulated liver B cells after Exo^{MSC} treatment. (B) Nuclear translocation of P65 by western blot of the cytoplasmic and nuclear fraction of αIgM/αCD40-stimulated B cells treated with Exo^{MSC}. (C) Western blot of p-IKKα/β, IKKα, IKKβ, p-Erk1/2, ERK1/2, and β-actin in LPS-stimulated liver B cells after Exo^{MSC} treatment. (D) Western blot of cytoplasmic and nuclear fractions of LPS-stimulated B cells treated with Exo^{MSC}. (E) Western blot of p-IKKα/β, IKKα, IKKβ, p-Erk1/2, ERK1/2, and β-actin following stimulation with PMA. (F) CFSE analyses of intrahepatic B cells in different groups. (G) mRNA levels of *Ccnd2* and *Ccne1* in B cells after stimulation with PMA (n = 4 for each group). (H) Western blot of expression levels of c-Myc, CCND2, and CCNE1 in B cells. (I) mRNA levels of *Tnf*, *Il6*, *Ccl2*, and *Ccl3* in B cells from different groups (n = 4 for each group). All data were presented as mean ± SEM. *$p < 0.05$, **$p < 0.01$, ***$p < 0.001$. Abbreviations: Ccl2, C-C motif chemokine ligand 2; CCND2, cyclin D2; CCNE1, cyclin E1; CFSE, 5,6-carboxyfluorescein diacetate succinimidyl ester; ERK, extracellular regulated kinase; Exo^{MSC}, MSC-derived exosomes; IKK, inhibitor of nuclear factor kappa-B kinase; LPS, lipopolysaccharide; MAPK, mitogen-activated protein kinase; MSC, mesenchymal stem cell; NF-kappa B, nuclear factor kappa B; PMA, phorbol 12-myristate 13-acetate.

Aa, *Traf4*, *Tnfrsf13c*, and *Traf1* when compared to those from fibrotic liver. Several pro-proliferative and pro-inflammatory signaling pathways were also inhibited by MSC treatment. This further elucidated the regulatory mechanism exerted by MSCs on B cells during LF.

B cell-deficient mice (μMT) and CD20-specific monoclonal antibody-treated mice are common animal models used to study B cell function in diseases.[15] Consistent with previous reports,[13–15] we observed significantly reduced fibrosis in both models. On the contrary, we found that the adoptive transfer of B cells markedly aggravated LF in CCl_4-treated μMT mice. This confirmed that the net effect of B-cell depletion is the amelioration of LF, providing evidence that B-cell activation in the liver is causative toward LF and not a bystander effect. Mechanistically, activated B cells may directly activate HSCs through pro-inflammatory cytokines or enhance the infiltration of CD11b^{hi} F4/80^{int} mononuclear macrophages

to further activate HSCs. Thus, targeting B-cell inhibition could be a potential therapeutic approach for managing LF. The administration of MSCs ameliorated exacerbated LF induced by the adoptive transfer of B cells, as demonstrated by the reduced expression levels of various fibrogenic markers following the co-injection of MSCs and B cells. From this perspective, MSC therapy holds greater potential for application compared to merely completely eliminating mature B cells from the entire body, as monoclonal antibody therapy may compromise normal humoral immune function, while MSCs specifically target abnormally activated B cells in the liver.

According to previous reports, human MSCs have significant inhibitory effects on the proliferation and differentiation of normal mature B cells isolated from peripheral blood.[33,34] In this study, we demonstrated that MSCs inhibit the function of intrahepatic B cells both in vivo and in vitro. The inhibition of intrahepatic B cell function by MSCs primarily relied on their secretome, as evidenced by the persistence of the inhibitory effect when we separated the two using a transwell culture system. The MSCs secretome is a spectrum of biologically active factors usually classified as cytokines, chemokines, cell adhesion molecules, lipid mediators, interleukins, growth factors, hormones, exosomes, and microvesicles.[35] The paracrine function of MSCs is partly mediated by exosomes, which contain abundant proteins, nucleic acids, and other bioactive molecules. A previous study demonstrated that the immunomodulatory effect of MSCs on B cells is independent of secreted extracellular vesicles.[36] However, another study reported that Exo^{MSC} could inhibit the proliferation and function of B cells.[37] These discrepant outcomes are believed to be mainly due to the significant variation in MSCs and B cell preparations obtained from diverse sources. We found that exosomes are involved in the inhibitory effect of MSCs on intrahepatic B cells. Exo^{MSC} effectively inhibited the activation, proliferation, and pro-inflammatory functions of intrahepatic B cells in vitro. The MAPK pathway plays an important role in regulating cell cycle entry and proliferation. In addition, the NF-kappa B pathway controls the transcription of DNA, cytokine production, and cell survival and plays a key role in regulating the inflammatory response. These 2 major signaling axes involved in intrahepatic B cell activation were inhibited by Exo^{MSC}, suggesting that Exo^{MSC} mainly targets the MAPK and NF-kappa B signaling pathways to suppress B cell function.

In summary, our data described in detail the characteristics of B cells in the progression of LF using scRNA-seq and demonstrated the therapeutic effect of MSCs by inhibiting intrahepatic B cell function, which might provide a potential target to treat LF. We also revealed that exosomes mediated the inhibitory effect of MSCs on B cells by regulating the MAPK and NF-kappa B signaling pathways. This study has vital implications in illustrating how MSC-mediated immunomodulatory effects on B cells are achieved during LF and lays a solid foundation for the application of MSCs in the treatment of LF.

DATA AVAILABILITY STATEMENT

The data for this study are available by contacting the corresponding author upon reasonable request.

AUTHOR CONTRIBUTIONS

Xudong Feng performed the experiments, analyzed the data, and drafted the manuscript. Bing Feng and Jiahang Zhou performed the experiments and analyzed the data. Jinfeng Yang, Qiaoling Pan, and Jiong Yu performed animal experiments and analyzed the data. Dandan Shang performed molecular experiments. Lanjuan Li conceived and directed the study. Hongcui Cao conceived and directed the study and critically revised the manuscript. All authors approved the final version to be published.

ACKNOWLEDGMENTS

The authors thank the staff of OE Biotech Co., Ltd (Shanghai, China) for their assistance with single-cell RNA sequencing analysis. They also thank Chao Bi from the Core Facilities, Zhejiang University School of Medicine, for her technical support. The schematic illustrations presented in this study were created with BioRender.com, and the authors thank them for their excellent tools.

FUNDING INFORMATION

This work was supported by National Key Research and Development Program of China (No. 2020YFA0113003), Key Research and Development Project of Zhejiang Province (No. 2023C03046), Fundamental Research Funds for the Central Universities (No. 2022ZFJH003), and Research Project of Jinan Microecological Biomedicine Shandong Laboratory (No. JNL-2023003C; No. JNL-2023005C).

CONFLICTS OF INTEREST

The authors have no conflicts to report.

ORCID

Xudong Feng https://orcid.org/0000–0002–4103–7737
Bing Feng https://orcid.org/0000–0002–2385–0417
Jiahang Zhou https://orcid.org/0000–0003–0623–517X
Jinfeng Yang https://orcid.org/0000–0001–6284–1700
Qiaoling Pan https://orcid.org/0000–0002–3771–8193
Jiong Yu https://orcid.org/0000–0002–1821–1178
Dandan Shang https://orcid.org/0009–0000–9675–8841
Lanjuan Li https://orcid.org/0000–0001–6945–0593
Hongcui Cao https://orcid.org/0000–0002–6604–6867

REFERENCES

1. Fallowfield JA. Therapeutic targets in liver fibrosis. Am J Physiol - Gastrointest Liver Physiol. 2011;300:G709–15.
2. Asrani SK, Devarbhavi H, Eaton J, Kamath PS. Burden of liver diseases in the world. J Hepatol. 2019;70:151–71.
3. Pellicoro A, Ramachandran P, Iredale JP, Fallowfield JA. Liver fibrosis and repair: Immune regulation of wound healing in a solid organ. Nat Rev Immunol. 2014;14:181–94.
4. Taylor AE, Carey AN, Kudira R, Lages CS, Shi T, Lam S, et al. Interleukin 2 promotes hepatic regulatory T Cell responses and protects from biliary fibrosis in murine sclerosing cholangitis. Hepatology. 2018;68:1905–21.
5. Tao X, Zhang R, Du R, Yu T, Yang H, Li J, et al. EP3 enhances adhesion and cytotoxicity of NK cells toward hepatic stellate cells in a murine liver fibrosis model. J Exp Med. 2022;219:e20212414.
6. Tacke F, Zimmermann HW. Macrophage heterogeneity in liver injury and fibrosis. J Hepatol. 2014;60:1090–6.
7. Karlmark KR, Weiskirchen R, Zimmermann HW, Gassler N, Ginhoux F, Weber C, et al. Hepatic recruitment of the inflammatory Gr1+ monocyte subset upon liver injury promotes hepatic fibrosis. Hepatology. 2009;50:261–74.
8. Ramachandran P, Pellicoro A, Vernon MA, Boulter L, Aucott RL, Ali A, et al. Differential Ly-6C expression identifies the recruited macrophage phenotype, which orchestrates the regression of murine liver fibrosis. Proc Natl Acad Sci USA. 2012;109:E3186–95.
9. Wehr A, Baeck C, Heymann F, Niemietz PM, Hammerich L, Martin C, et al. Chemokine receptor CXCR6-dependent hepatic NK T Cell accumulation promotes inflammation and liver fibrosis. J Immunol. 2013;190:5226–36.
10. Park O, Jeong W Il, Wang L, Wang H, Lian ZX, Gershwin ME, et al. Diverse roles of invariant natural killer T cells in liver injury and fibrosis induced by carbon tetrachloride. Hepatology. 2009; 49:1683–94.
11. Shen H, Sheng L, Xiong Y, Kim YH, Jiang L, Chen Z, et al. Thymic NF-κB-inducing kinase regulates CD4+ T cell-elicited liver injury and fibrosis in mice. J Hepatol. 2017;67:100–9.
12. Lukacs-Kornek V, Schuppan D. Dendritic cells in liver injury and fibrosis: Shortcomings and promises. J Hepatol. 2013;59:1124–6.
13. Novobrantseva TI, Majeau GR, Amatucci A, Kogan S, Brenner I, Casola S, et al. Attenuated liver fibrosis in the absence of B cells. J Clin Invest. 2005;115:3072–82.
14. Thapa M, Chinnadurai R, Velazquez VM, Tedesco D, Elrod E, Han JH, et al. Liver fibrosis occurs through dysregulation of MyD88-dependent innate B-cell activity. Hepatology. 2015;61:2067–79.
15. Faggioli F, Palagano E, Di Tommaso L, Donadon M, Marrella V, Recordati C, et al. B lymphocytes limit senescence-driven fibrosis resolution and favor hepatocarcinogenesis in mouse liver injury. Hepatology. 2018;67:1970–85.
16. Zhang F, Jiang WW, Li X, Qiu XY, Wu Z, Chi YJ, et al. Role of intrahepatic B cells in non-alcoholic fatty liver disease by secreting pro-inflammatory cytokines and regulating intrahepatic T cells. J Dig Dis. 2016;17:464–74.
17. Barrow F, Khan S, Fredrickson G, Wang H, Dietsche K, Parthiban P, et al. Microbiota-driven activation of intrahepatic B Cells aggravates NASH through innate and adaptive signaling. Hepatology. 2021;74:704–22.
18. Pai M, Spalding D, Xi F, Habib N. Autologous bone marrow stem cells in the treatment of chronic liver disease. Int J Hepatol. 2012;2012:1–7.
19. Watanabe Y, Tsuchiya A, Seino S, Kawata Y, Kojima Y, Ikarashi S, et al. Mesenchymal stem cells and induced bone marrow-derived macrophages synergistically improve liver fibrosis in mice. Stem Cells Transl Med. 2019;8:271–84.
20. Milosavljevic N, Gazdic M, Simovic Markovic B, Arsenijevic A, Nurkovic J, Dolicanin Z, et al. Mesenchymal stem cells attenuate liver fibrosis by suppressing Th17 cells – An experimental study. Transpl Int. 2018;31:102–15.
21. Ramachandran P, Matchett KP, Dobie R, Wilson-Kanamori JR, Henderson NC. Single-cell technologies in hepatology: New insights into liver biology and disease pathogenesis. Nat Rev Gastroenterol Hepatol. 2020;17:457–72.
22. Kitamura D, Roes J, Kühn R, Rajewsky KA. B cell-deficient mouse by targeted disruption of the membrane exon of the immunoglobulin μ chain gene. Nature. 1991;350:423–6.
23. Uchida J, Lee Y, Hasegawa M, Liang Y, Bradney A, Oliver JA, et al. Mouse CD20 expression and function. Int Immunol. 2004;16:119–29.
24. Ehling J, Bartneck M, Wei X, Gremse F, Fech V, Möckel D, et al. CCL2-dependent infiltrating macrophages promote angiogenesis in progressive liver fibrosis. Gut. 2014;63:1960–71.
25. Ren G, Zhang L, Zhao X, Xu G, Zhang Y, Roberts AI, et al. Mesenchymal Stem cell-mediated immunosuppression occurs via concerted action of chemokines and nitric oxide. Cell Stem Cell. 2008;2:141–50.
26. Liu J, Li P, Zhu J, Lin F, Zhou J, Feng B, et al. Mesenchymal stem cell-mediated immunomodulation of recruited mononuclear phagocytes during acute lung injury: A high-dimensional analysis study. Theranostics. 2021;11:2232–46.
27. Ghasemi M, Roshandel E, Mohammadian M, Farhadihosseinabadi B, Akbarzadehlaleh P, Shamsasenjan K. Mesenchymal stromal cell-derived secretome-based therapy for neurodegenerative diseases: Overview of clinical trials. Stem Cell Res Ther. 2023;14:122.
28. Henderson NC, Rieder F, Wynn TA. Fibrosis: From mechanisms to medicines. Nature. 2020;587:555–66.
29. Hammerich L, Tacke F. Hepatic inflammatory responses in liver fibrosis. Nat Rev Gastroenterol Hepatol. 2023;20:633–46.
30. Jagannathan M, Hasturk H, Liang Y, Shin H, Hetzel JT, Kantarci A, et al. TLR cross-talk specifically regulates cytokine production by B cells from chronic inflammatory disease patients. J Immunol. 2009;183:7461–70.
31. Shi Y, Hu G, Su J, Li W, Chen Q, Shou P, et al. Mesenchymal stem cells: A new strategy for immunosuppression and tissue repair. Cell Res. 2010;20:510–8.
32. Bai YM, Yang F, Luo P, Xie LL, Chen JH, Guan YD, et al. Single-cell transcriptomic dissection of the cellular and molecular events underlying the triclosan-induced liver fibrosis in mice. Mil Med Res. 2023;10:7.
33. Corcione A, Benvenuto F, Ferretti E, Giunti D, Cappiello V, Cazzanti F, et al. Human mesenchymal stem cells modulate B-cell functions. Blood. 2006;107:367–72.
34. Tabera S, Pérez-Simón JA, Díez-Campelo M, Sánchez-Abarca LI, Blanco B, López A, et al. The effect of mesenchymal stem cells on the viability, proliferation and differentiation of B-lymphocytes. Haematologica. 2008;93:1301–9.
35. PK L, Kandoi S, Misra R, V S, R K, Verma RS. The mesenchymal stem cell secretome: A new paradigm towards cell-free therapeutic mode in regenerative medicine. Cytokine Growth Factor Rev. 2019;46:1–9.
36. Carreras-Planella L, Monguió-Tortajada M, Enric Borràs F, Franquesa M. Immunomodulatory effect of MSC on B cells is independent of secreted extracellular vesicles. Front Immunol. 2019;10:1288.
37. Khare D, Or R, Resnick I, Barkatz C, Almogi-Hazan O, Avni B. Mesenchymal stromal cell-derived exosomes affect mRNA expression and function of B-lymphocytes. Front Immunol. 2018;9:3053.

How to cite this article: Feng X, Feng B, Zhou J, Yang J, Pan Q, Yu J, et al. Mesenchymal stem cells alleviate mouse liver fibrosis by inhibiting pathogenic function of intrahepatic B cells. Hepatology. 2025;81:1211–1227. https://doi.org/10.1097/HEP.0000000000000831